Presented at Conference on
Particle Physics, Irvine, Ca,
Dec. 3-4, 1971

LBL-788
Preprint

RESONANCES AND SYMMETRIES

Arthur H. Rosenfeld

April 1972

AEC Contract No. W-7405-eng-48

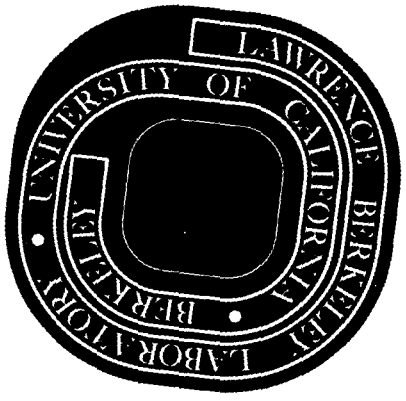

LBL-788

DISCLAIMER

RESONANCES AND SYMMETRIES

Arthur H. Rosenfeld
Department of Physics, and
Lawrence Berkeley Laboratory
University of California
Berkeley, California 94720

ABSTRACT

In baryon phenomenology we discuss mainly a recent paper paper by G. H. Trilling on SU(3) tests. He shows that SU(3) predictions relating cross sections can be greatly improved by the introduction of angular momentum barrier penetration coefficients, as is already routine when making SU(3) classifications of resonances.

Under mesons we discuss $\pi\pi$ and $K\pi$ s-wave scattering. The recent work of Flatté et al. and of Protopopescu et al. explains s-wave $\pi\pi$ scattering in terms of two poles:

$$\epsilon \text{ at } \sqrt{s} = 600 \pm 70 - i(250 \pm 50) \text{ MeV on sheets II or IV,}$$

$$S^* \text{ at } \sqrt{s} = 980 \pm 7 - i(38 \pm 7) \text{ MeV on sheet II.}$$

INTRODUCTION

The program chairman asked me to choose one current interesting advance in our understanding of baryons, and one advance in mesons. For my baryon topic I have chosen to point out the success of a nice and simple paper by G. H. Trilling which greatly improves the agreement between experimental cross sections and SU(3) predictions.

For my meson topic I have chosen the recent rapid advance in our understanding of s-wave $\pi\pi$ and $K\pi$ scattering amplitudes, with $\pi\pi$ poles called ϵ at ~ 600 MeV and S^* at $\bar{K}K$ threshold, and several possible $K\pi$ poles.

I. TESTS OF SU(3) IN PARTICLE REACTIONS

I want to start by contrasting two familiar figures involving SU(3) predictions: one shows the success of scaling decay rates; one shows the failure to relate cross sections. Figure 1, is taken from the review of Tripp et al.[1] The left panel shows SU(3) coupling constants g (actually what is plotted is g^2) calculated for a total of four different decay rates of three different resonances which are members of the same $J = 3/2^+$ decuplet. If SU(3) were perfectly described by our Eq. (3) below, which applies for decays, then the same value of g^2 would describe all four decays. It can be seen that SU(3) "succeeds," on the average, to better than ± 50%. Other panels of Fig. 1 confirm this.

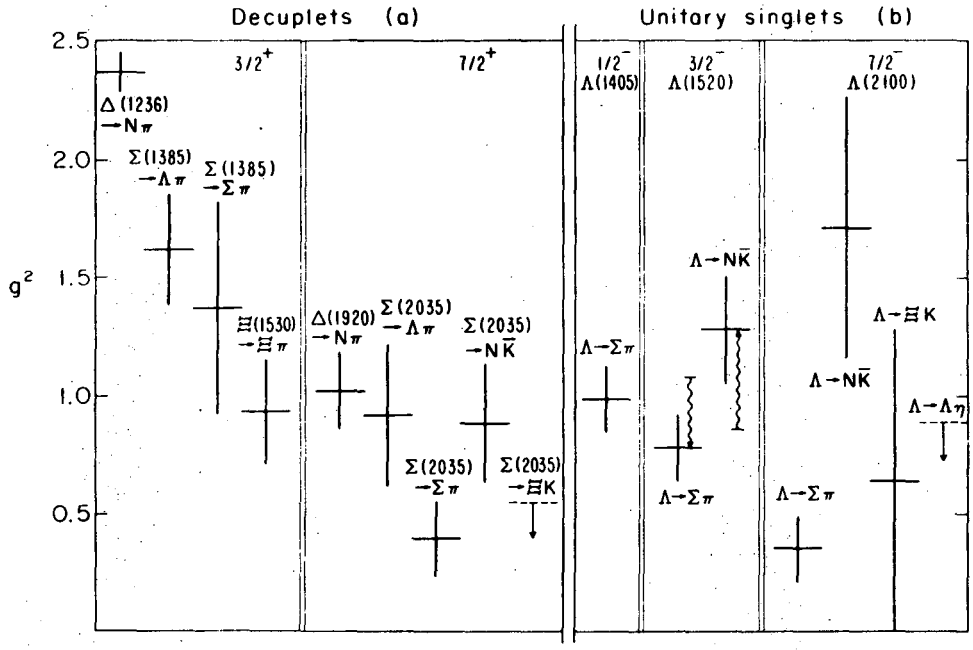

Fig. 1. Display of the relative coupling constants for (a) various decay modes of the $3/2^+$ decuplet and its recurrence and (b) the $1/2^-$ unitary singlet and the $3/2^-$ unitary singlet and its recurrence. The SU(3) coefficients and corrections for mass differences have been introduced so that within each multiplet all decay modes should have the same value of g^2. Taken from R. D. Tripp, et al., Nucl. Phys. B3, 10 (1967).

Figure 2 shows the SU(3) matrix element T (actually what is plotted is $|T|^2$) calculated by Meshkov, Snow, and Yodh[2] for four different reactions. If SU(3) were perfectly described by our Eq. (8) below, then the same T would describe all four reactions. Instead, $|T|^2$ for the endothermic reactions (involving K^+ production), lie one or more orders of magnitude below those like $K^-p \to Y_1^*(1386)\pi$, which is endothermic by only 100 MeV.

Why does Eq. (3) work for resonance decays, while Eq. (8) fails for cross sections? The answer, recently given by Trilling[3] is that Eq. (3) includes an extra centrifugal barrier-penetration factor B_ℓ. Thus, for the p-wave decay of the $3/2^+$ decuplet of Fig. 1, the factor is

$$B_1(kR) = \frac{(kR)^2}{1 + (kR)^2} ,$$

where k is the decay momentum and R is the radius of interaction. Specifically for the lowest-Q decay of Fig. 1, $\Sigma(1385) \to \Sigma\pi$, $kR = 117$ MeV/c ≈ 1 fermi ≈ 0.5, and $B_1 \sim 1/3$, which is an appreciable and necessary correction, the like of which we shall now incorporate into cross sections.

Calculation of SU(3) Couplings

Having introduced you to the barrier problem, I want now to summarize how from data one extracts, or can extract, SU(3) couplings or reduced widths for three different cases:

A. Decay rates of resonances with known quantum numbers.

B. Cross sections where partial wave analyses are available.

C. Cross sections where little is known.

A. Decays of Resonances with Known Quantum Numbers

Here the procedure is well standardized. I take a few paragraphs from Appendix II of the forthcoming Review of Particle Properties,[4] where an up-to-date list of references may also be found.

Decay Rates

In terms of a relativistically invariant matrix element T, the decay rate for two-body decay of a resonance of mass M is

$$\Gamma \propto \frac{|T|^2 R_2}{M} , \qquad (1)$$

where $R_2 = k/M$ is the two-body phase space factor. Since the numerator is an invariant, and since Γ must transform as $1/E$, we

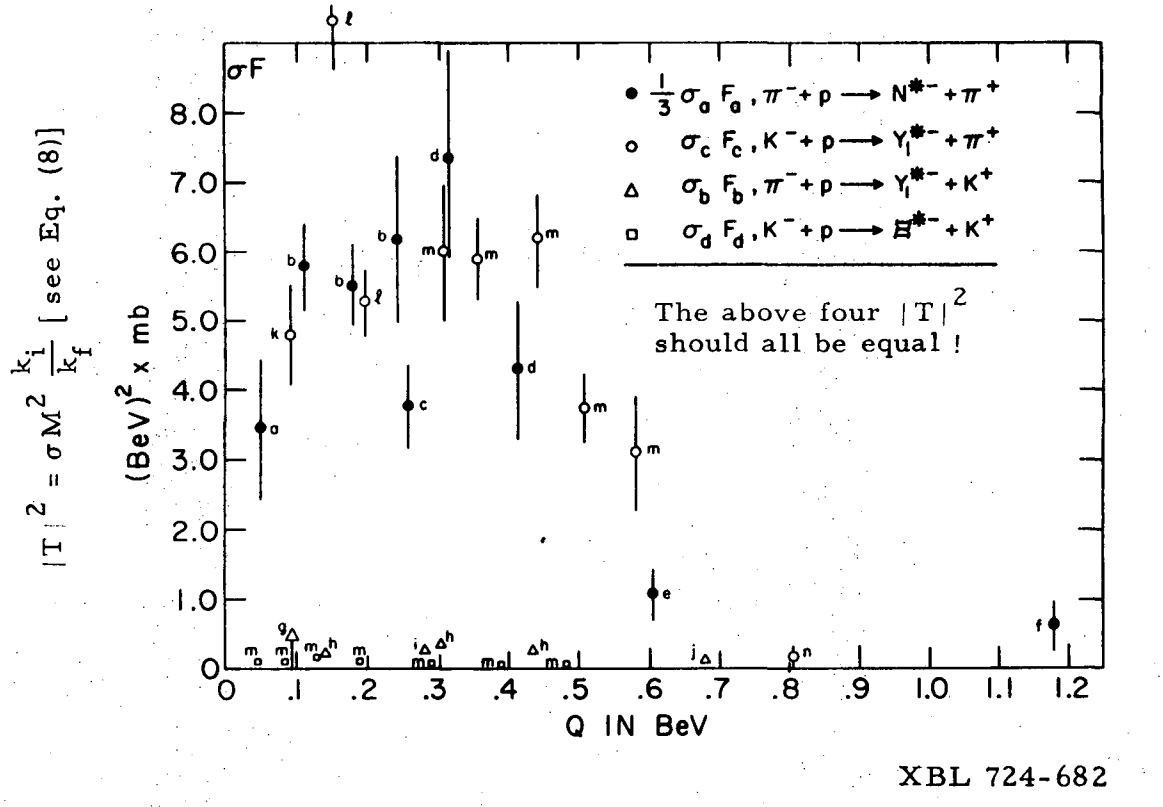

Fig. 2. Experimental values of $1/3\ \sigma_a F_a$, $\sigma_b F_b$, $\sigma_c F_c$, and $\sigma_d F_d$ vs Q for the "U-spin equalities." The letter next to each data point is the reference number of the data source. This is Fig. 2 of Meshkov, Snow, and Yodh, Phys. Rev. Letters 13, 212 (1964).

introduce the denominator 1/M.

For meson decays (see below) the rates are calculated according to Eq. (1); for baryon resonance decays into $1/2^+$ baryons and 0^- mesons, one next takes into account the fact that spin sums in $|T|^2$ introduce another factor M cancelling the 1/M. We are then left with

$$\Gamma = \frac{|T|^2 k}{M} M_N, \text{ for baryons} \tag{2}$$

$$= \frac{|T|^2 k}{M^2} M_N^2, \text{ for mesons.} \tag{2'}$$

The powers of the nucleon mass M_N or M_N^2 have been introduced so that we can treat $|T|$ as dimensionless.

$|T|^2$ contains centrifugal barrier factors, which we call B_ℓ. We then have

$$\left.\begin{matrix}\text{Decuplet} \\ \text{Singlet}\end{matrix}\right\} \quad \Gamma = (cg)^2 B_\ell(k) \frac{M_N}{M} k \tag{3}$$

$$\text{Octet} \qquad \Gamma = (c_D g_D + c_F g_F)^2 B_\ell(k) \frac{M_N}{M} k \tag{4}$$

$$\left.\begin{matrix}\text{Octet-} \\ \text{Singlet} \\ \text{mixing}\end{matrix}\right\} \quad \begin{cases} G_8 = \Lambda \cos\theta - \Lambda' \sin\theta \\ G_1 = \Lambda \sin\theta + \Lambda' \cos\theta \end{cases} \tag{5}$$

$$\text{with} \quad \begin{aligned} G_8 &= c_D g_D + c_F g_F \\ G_1 &= c_1 g_1 \,. \end{aligned} \tag{6}$$

Here c_i are the SU(3) coefficients with the sign convention adopted in this article. M_N is the nucleon mass, M is the resonance mass for which Γ is calculated, k is the center-of-mass momentum for the channel being considered, g_i are the relevant couplings.

The appendix goes on to discuss singlet-octet mixing, which we can ignore, except to say that when it is taken into account, we find that the g_i for the octets agree as well as they did for the decuplets and singlets pictured in Fig. 1. Progress for the resonances classified as of 1969 is summarized by Levi-Setti[5] in my Fig. 3, where the standard deviation of the observed g_i seems to be $\approx \pm 50\%$.

Next we come to cross sections, e.g., $K^- p \to \Lambda\pi$, where we call $K^- p$, channel 1; $\Lambda\pi$, channel β. Then, using the same notation as in Eq. (2),

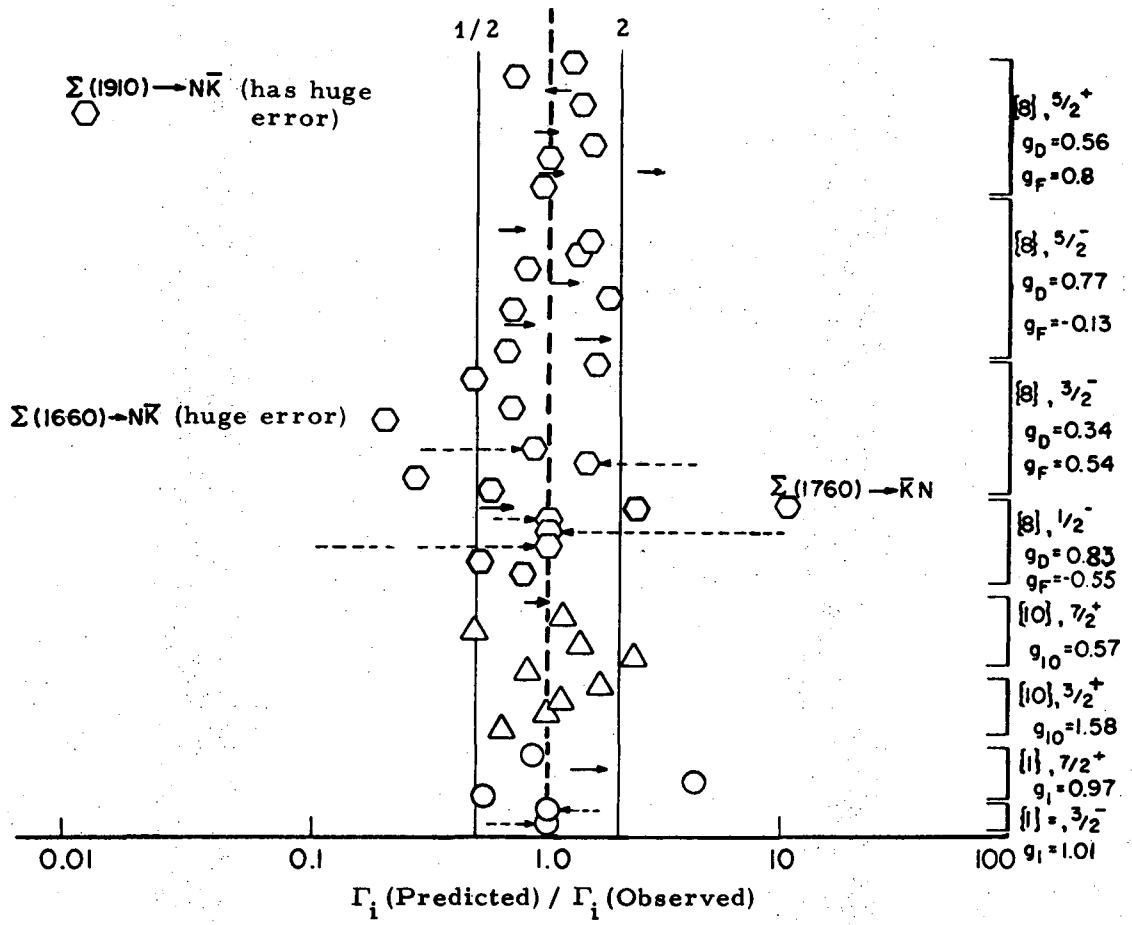

Fig. 3. By defining as "predicted" widths, those predicted using the best values for the SU(3) multiplet coupling constants, the ratios of the predicted width to observed width are indicated for the decay modes and SU(3) assignments entered in Levi-Setti's Table 3. The tails of solid arrows correspond to the locations of upper or lower limits of decay rates. The dashed arrows indicate the displacement caused by the introduction of singlet-octet mixing in the $1/2^-$ and $3/2^-$ states. This is Fig. 3 of Levi-Setti's talk at the 1969 Lund Intl. Conf. on Elementary Particles. Proceedings published by Institute of Physics, Lund, Sweden.

$$\Gamma_{1\beta} = \sigma_{1\beta} f = |T_{1\beta}|^2 \frac{k_\beta}{M} M_N , \tag{7}$$

where f is the flux factor ($f \propto k_1 M$, where both f_1 and f_β are expressed in the c. m. and $M = \sqrt{s}$). This gives immediately

$$\sigma_{1\beta} = \frac{|T_{1\beta}|^2}{s} \frac{k_\beta}{k_1} \equiv |T_{1\beta}|^2 / F_{MSY} , \tag{8}$$

which is the equation used in 1964 by Meshkov, Snow, and Yodh to plot the $|T|^2$ of Fig. 2. They would have been more successful if they had taken one more step, written something like

$$T_{1\beta}^{(\ell)} = c_1 g_1 \sqrt{B_\ell (k_1 R)} \; c_\beta g_\beta \sqrt{B_\ell (k_\beta R)} , \tag{9}$$

and then plotted $g_1 g_\beta$.

However, before lamenting lost barrier factors, and before leaving the success of SU(3) for resonances, I want to remind you of the current successful sign count associated with Eq. (9). Assume that our reaction goes through a resonant intermediate state:

$$K^- p \rightarrow \text{Res}(M) \rightarrow \Lambda\pi ,$$

where in fact Res(M) is one of the six Σ resonances labelled in my Fig. 4. Note that the initial and final states (K^-p and $\Lambda\pi$) are, from the point of view of SU(3), closely related; i. e., π and K belong to the same 0^- octet, p and Λ to the same $1/2^+$ octet. This means that we are really discussing "SU(3)-elastic" scattering:

$$0^- \times 1/2^+ \xrightarrow{g_1} \text{Res}(M) \xrightarrow{g_\beta} 0^- \times 1/2^+$$

so that g_1 and g_β are both the <u>same</u> SU(3) coupling constant $g[0^-, 1/2^+, \text{Res}(M)]$ and

$$T = c_1 c_\beta g^2 \sqrt{B_1 B_\beta} . \tag{10}$$

Hence the sign of T should be just the sign of the product $c_1 c_\beta$ of the SU(3) and SU(2) coefficients. Experimentally the intermediate resonances overlap in energy enough to permit a measurement of the sign of the $\Lambda\pi$ interference. Figure 4 shows 19 resonances whose interferences permit 16 sign checks, 15 of which have actually been checked. Since 2^{15} is a very large number, I find this a glorious victory for SU(3).

I conclude that for case A [SU(3) applied to <u>resonances</u>], SU(3) relates hundreds of measurements in a very satisfactory way.

SU(3) RELATIVE SIGN OF RESONANT AMPLITUDES

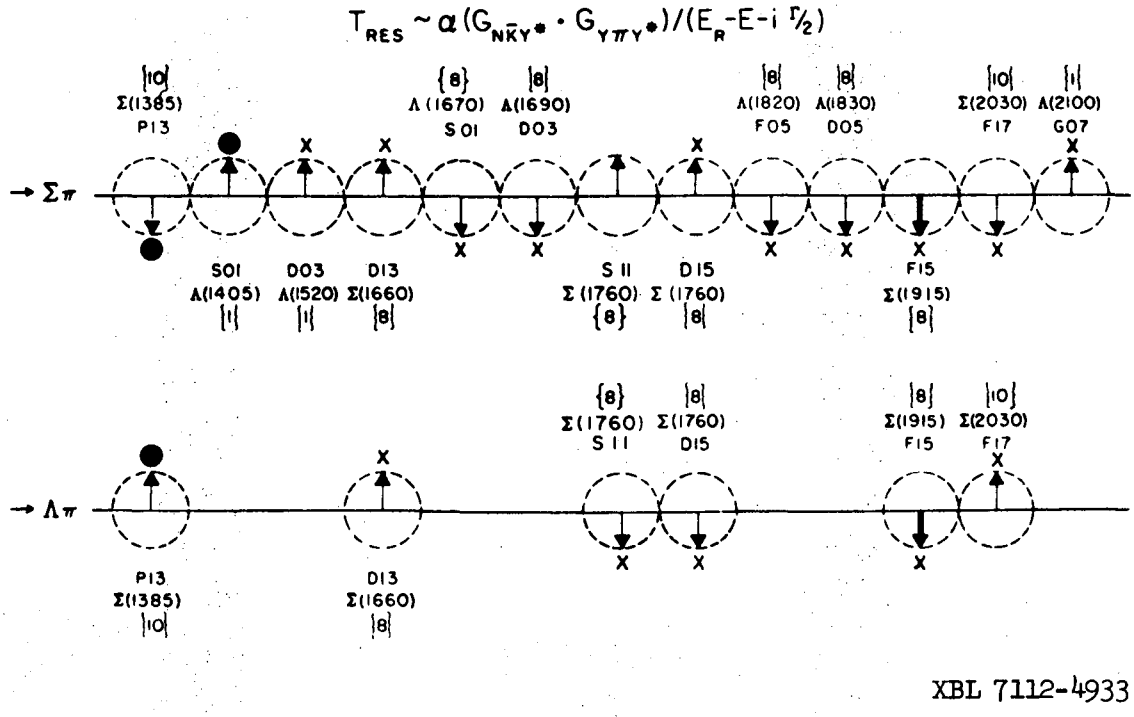

Fig. 4. Plot reproduced from Levi-Setti's review at Lund, 1969. Arrows indicate the sign of the amplitude predicted from Eq. (10); X marks the observed phases. Three phases are arbitrary (one for each final state: $\Lambda\pi$, $\Sigma\pi$ in $I = 0$, $\Sigma\pi$ in $I = 1$) and are indicated with black dots.

A Discussion of Barrier Penetration Factors B_ℓ

Before going on to introduce the centrifugal barrier-penetration factors B_ℓ (with ℓ up to 10) into the cross-section equation (18), we had better discuss the factors themselves and introduce you to both the standard reference [Chap. VIII of Blatt and Weisskopf's Theoretical Nuclear Physics (John Wiley, 1952)] and to a nice and convenient new treatment by von Hippel and Quigg,[16]

The "industry standard" for B_ℓ is taken from Blatt and Weisskopf's Eq. (5.8), page 361, where they are called v_ℓ:

$$B_0 = 1, \quad B_1 = \frac{x^2}{1+x^2}, \quad B_2 = \frac{x^4}{9+3x^2+x^4}, \cdots \tag{10.1}$$

where $x = kR$ as used above. For $x << \ell$,

$$B_\ell \xrightarrow{x \to 0} \frac{x^{2\ell}}{[(2\ell-1)!!]^2} \tag{10.2}$$

and for $x >> \ell$, $B_\ell \to 1$. Figure 5 gives B_ℓ vs. kR for 1 – 7.

I have always found the Blatt and Weisskopf treatment slightly unsatisfactory for two reasons:

1) It assumes that the region of interaction is a square well and matches the logarithmic derivative of the wave functions at the boundary. That's fine when the intermediate state is a nucleus; but I find it a bit disconcerting when it is, say, $\Delta(1236)$.

2) I could understand that the essence of the problem involved the properties of the spherical Bessel functions j_ℓ, or more precisely of the outgoing spherical Hankel functions h_ℓ

$$h_\ell = \sqrt{\frac{\pi}{2x}}\,[j_\ell(x) + i\eta_\ell(x)]. \tag{11}$$

But the relation of the B_ℓ to $|h_\ell|^2$ was not perfectly transparent.

Von Hippel and Quigg have eased both my dissatisfactions. Without any matching of wave functions, they merely note that outside R, where the only potential is the centrifugal barrier, the radial wave function $U(x) = r\psi(x)$ is given by

$$U_\ell(x) = Cx\,h_\ell(x) \tag{12}$$

where C is a normalization constant.

For large x ($>> \ell$), $|U|$ approaches a constant,

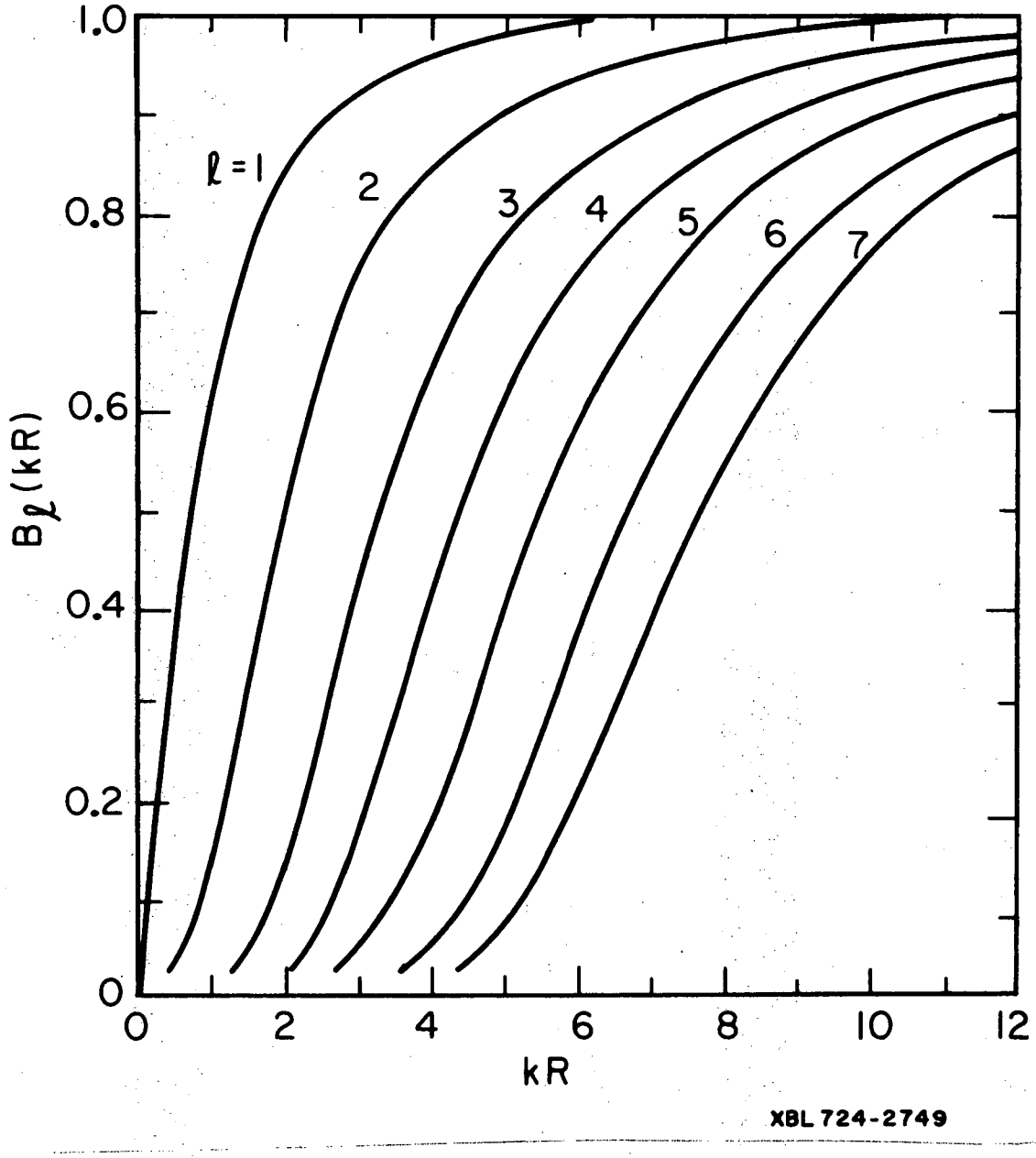

Fig. 5. Barrier factors B_ℓ from Eqs. (15) or (16) which also corresponds to the v_ℓ of Blatt and Weisskopf (Eq. 5.8, page 361). To get the full kinematic part of the partical width one must still include a two-body phase space factor k/M, as in Eq. (3).

$$U_\ell(x) = C \exp\left[i\left(x - \frac{\ell\pi}{2}\right)\right] , \tag{13}$$

but inside of $x = \ell$, Eq. (12) increases rapidly with decreasing x. The reason, they point out, is that the outgoing wave is being reflected inwards by the centrifugal barrier. The quantity of interest comes by dividing (12) by (13) to give

$$\left|\frac{U_\ell(kR)}{U_\ell(\infty)}\right| = xh_\ell(x) \Big|_{kR} = kR\, h_\ell(kR) . \tag{14}$$

This is the amplitude at R required to "push" one unit out to $r = \infty$. They then get B_ℓ by squaring Eq. (14) and taking its reciprocal. They call it the transmission coefficient T, but I have already used "T" for a T matrix element, so I write

$$B_\ell = \frac{1}{\left| kR\, h_\ell\,(kR)\right|^2} . \tag{15}$$

Their transmission coefficients B_ℓ are identically the v_ℓ of Blatt and Weisskopf, which should settle any doubts about the original derivation. These dimensionless B_ℓ are then related to the T matrix elements of Eqs. (2) and (7) by Eq. (3) as before:

$$\Gamma = (cg)^2\, B_\ell\, \frac{k}{M}\, M_N . \tag{3}$$

Von Hippel and Quigg like to call $B_\ell k/M$ the "kinematic width."

In an Appendix, von Hippel and Quigg give a useful power series expansion for the h_ℓ; however Tom Lasinski has pointed out to me that their power series involves complex arithmetic, and there is an even simpler real expression[7] for the $|h_\ell|^2$:

$$\left| xh_\ell(x)\right|^2 = \sum_{k=0}^{\ell} \frac{(2\ell-k)!\ (2\ell-2k)!}{k!\ [\ (\ell-k)!\ ]^2}\ (2x)^{2(k-\ell)} \tag{16}$$

Von Hippel and Quigg take up the question of the best value for R, from several points of view:

1. The shape of resonances, e.g. $\Delta(1236)$.

2. SU(3) relations between the widths of resonances, as in Fig. 1.

3. Lower limits on R. This is based on the observation that the amplitude in (14) must not become so large in the region outside R that it leads to a probability greater than unity.

Their conclusion is:

for meson resonances, $1/4\ F < R < 3/4\ F$;

for baryon resonances, $1/2\ F < R < 1\ F$.

There are several other nice physics points in their paper, but we must now return to the calculation of SU(3) coupling constants from cross sections.

B. Cross Sections Where a Partial Wave Analysis Is Available

B1. First consider two reactions fed by the same incoming state.

Trilling choses two which should, according to SU(3), be equal:

$$K^- p \to \pi^+ \Sigma^- \text{ (exothermic, and partial wave analysis available),} \tag{17}$$

$$\to K^\circ \equiv {}^\circ \text{ (endothermic, no partial wave analysis available).} \tag{18}$$

Figure 6 (Trilling's Fig. 3) shows that the observed exothermic cross section is larger than the endothermic one by an order of magnitude. He then explains the ratio with the help of the thesis of Dan Kane,[8] who did the partial wave analysis of $K^- p \to \pi^+ \Sigma^-$.

To discuss the scaling, we combine Eqs. (8) and (9) and generalize the result to a sum over partial waves

$$\frac{d\sigma}{d\omega} = \frac{1}{s} \left| \sum_\ell (2j+1)\, T^\ell_{1\beta}\, P_\ell(\theta) \right|^2 \frac{k_\beta}{k_1} \tag{19}$$

$$= \frac{1}{s} \left| \Sigma\, (2j+1)\, c_1 g_1 c_\beta g_\beta \sqrt{B_\ell(k_1) B_\ell(k_\beta)}\, P_\ell \right|^2 \frac{k_\beta}{k_1} .$$

If we had a partial wave decomposition of both reactions (17) and (18), we could factor out all the kinematics and SU(3) coefficients and compare g_{17} and g_{18}. But for the case in hand we can only predict (18) from (17). To do this, write (19) exhibiting only those factors which depend on k_β

$$\frac{d\sigma}{d\omega} = \frac{1}{s} \left| \Sigma\, (2j+1)\, \tau^\ell_{1\beta} \sqrt{k_\beta B_\ell(k_\beta)}\; P_\ell \right|^2 \frac{1}{k_1} . \tag{20}$$

Where $\sqrt{k_\beta B_\ell(k_\beta)}$ accounts for both phase space and B_ℓ.

The τ should then be the same for both reactions, so we can predict the second from the first just by changing the value of k_β in (20).

The result of this scaling is Trilling's Figs. 3 and 4, which are my Figs. 6 and 7. Figure 6 shows the cross sections vs. energy. The top curve [through $\sigma(\pi\Sigma)$] is Kane's partial-wave fit.

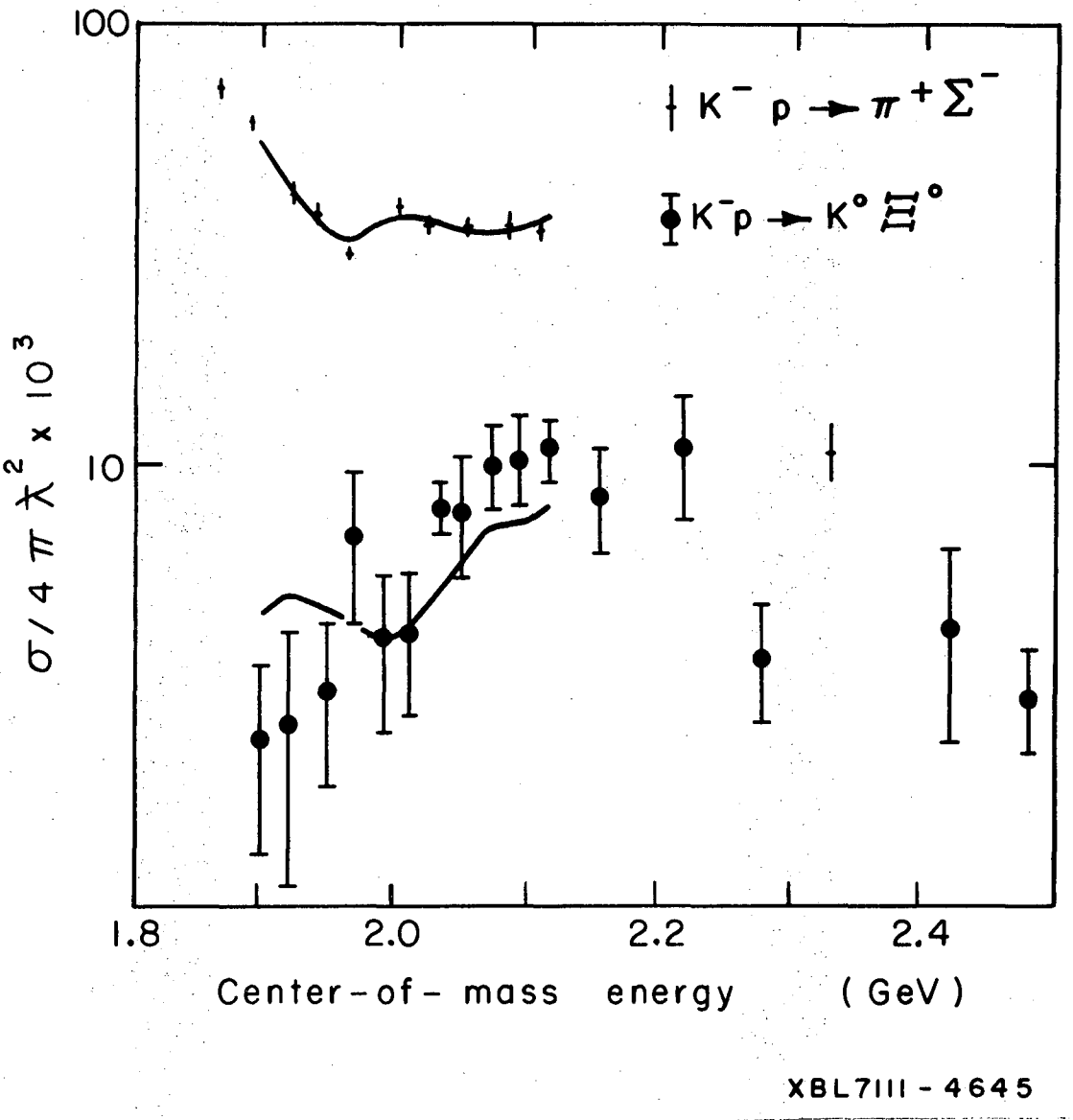

Fig. 6. Trilling's comparison of two K^-p cross sections. Top curve is from fit B2 of Kane's thesis. Bottom curve is top curve scaled according to Eq. (20). This is Fig. 3 of Trilling.[3]

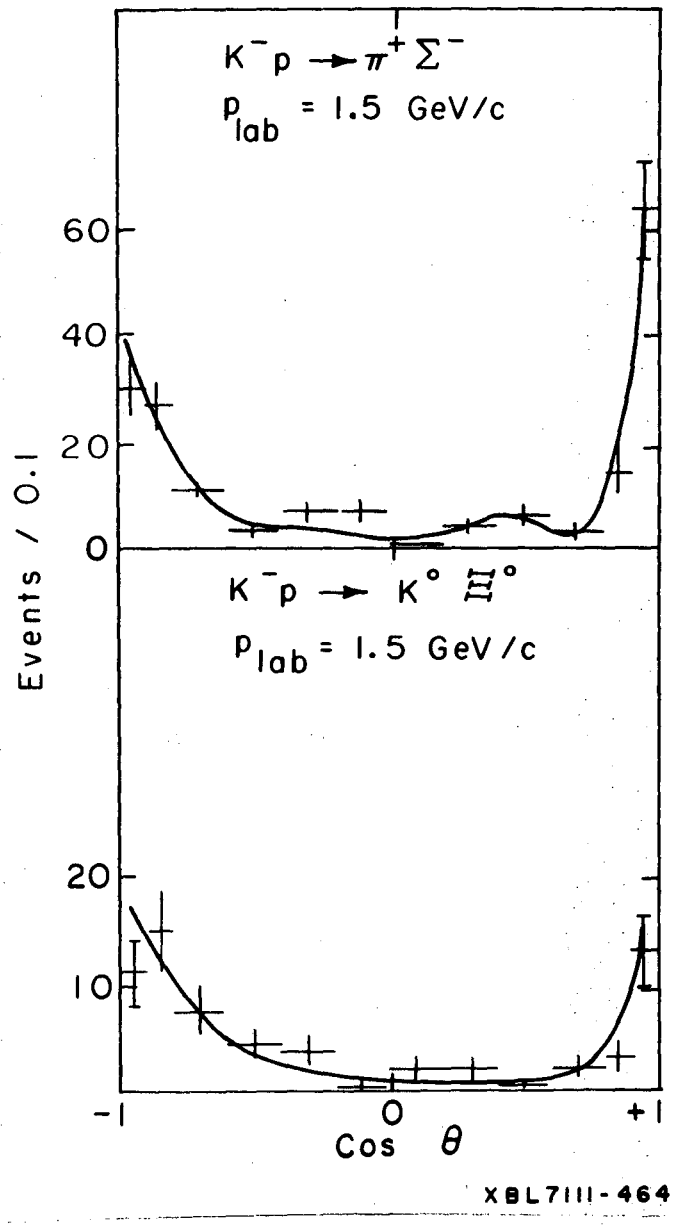

Fig. 7. Trilling's comparison of two K^-p angular distributions.

The lower curve is the top curve scaled down according to (20). The agreement is good. Figure 7 does the same scaling for the angular distributions at one energy ($\sqrt{s}$ = 1930 MeV), again with considerable success.

B2. Reactions fed by different states.

Our previous example involved only one initial state, so it made sense to compare the two reactions at the same value of s, i.e. the same value of P_{beam}.

Trilling next considers another pair of cross sections which SU(3) says should be equal:

$$\pi^- p \rightarrow K^+ \Sigma^- \tag{21}$$

$$K^- n \rightarrow K^0 \Xi^- \tag{22}$$

At what energies shall we make the comparison? If we could identify resonances, we might compare at the peak of corresponding resonances. Since $\bar{K}N$ resonances are heavier than their πN counterparts in the same supermultiplet, perhaps we should compare at the same incoming momenta. Actually, I made a table of corresponding N^* and Y^* resonances, and compared both their decay momenta into πN or $\bar{K}N$, and also the π or $\bar{K}$ beam momentum needed to form them. The kinematic quantity that matches as well or better than any other is the beam momentum. This is exactly the choice that Trilling made on the grounds of convenience, and he finds that it works well.

C. Effective ℓ for Cross Sections Where No Partial Wave Analysis Is Known

For such cross sections a new question arises: what average or effective angular momentum ℓ shall we chose for the barrier factors B_ℓ? Trilling follows the procedure of Davier and Harari.[9]

C1. For channels where nonexotic particles can be exchanged: e.g., $\pi^+ p \rightarrow K^+ \Sigma^+$.

At small t these should be dominated by a peripheral term of the form $J_0(R\sqrt{-t}) = J_0(R\ 2k \sin\theta)$ which corresponds to $\ell = kR$. He chooses R so as to make the first zero of $J_0[J_0(2.4) = 0]$ correspond to the cross-over between $\pi^+ p$ and $K^+ p$ differential cross sections, namely at $-t = 0.3$ GeV^2. Then $R \times \sqrt{0.3} = 2.4$, which gives R = 0.88 F, and

$$\ell = kR = k \times 0.88\ F = \frac{k(MeV)c}{225}. \tag{23}$$

I wondered if this radius seems reasonable at lower energy, where direct-channel resonances produce bumps in the cross section, so I made Fig. 8, which is a scatter plot of all the πN resonances on

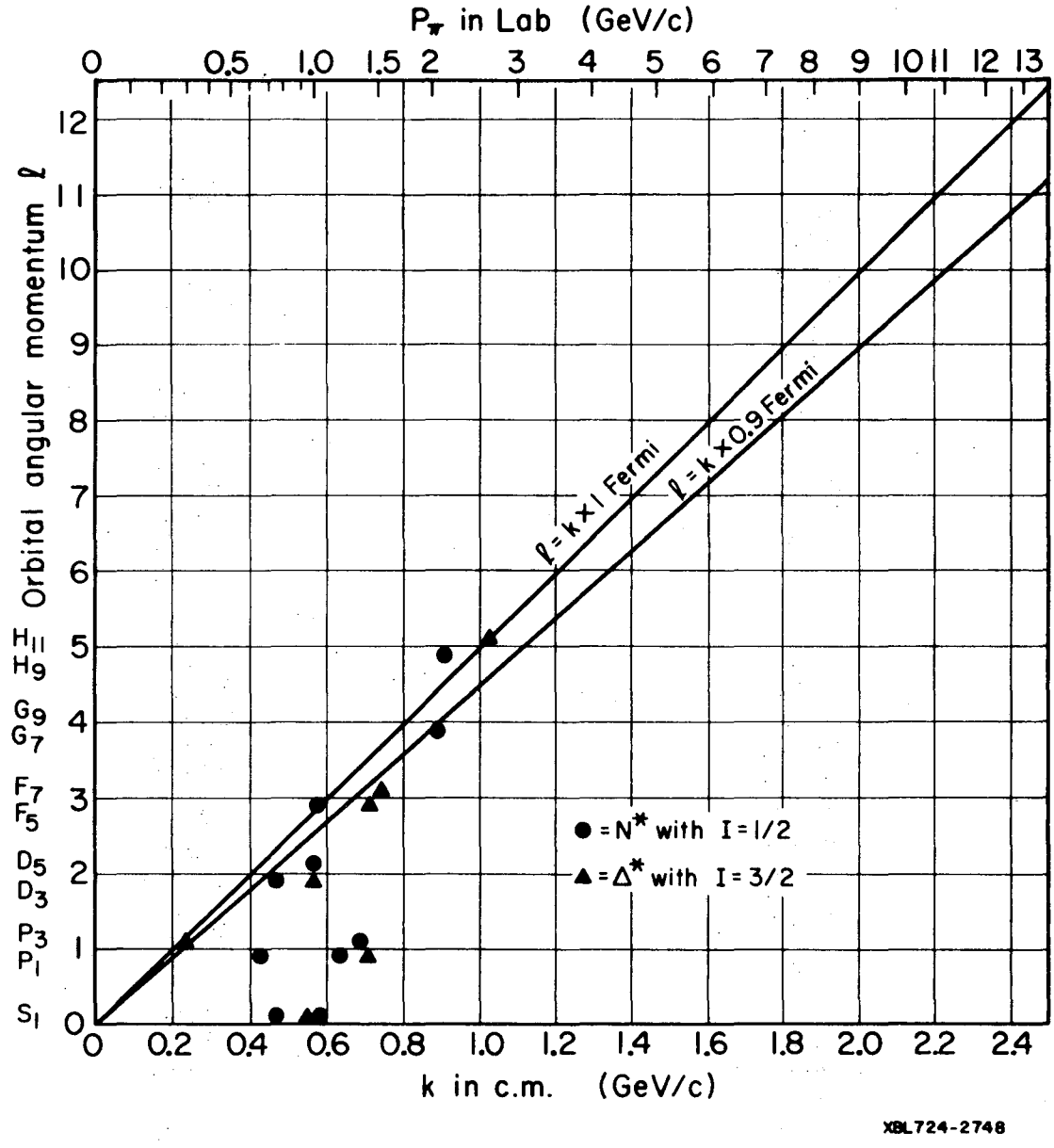

Fig. 8. Scatter plot of the known non-strange resonances. The lower x-scale is the c. m. momentum of the Nπ decay mode. The upper scale, for convenience, is the pion lab momentum necessary to form the resonance.

the particle data tables. All the dots fall on or below a line given by

$$\ell_{max} = k \times 1 \text{ fermi} = \frac{k(\text{MeV}/c)}{200}. \qquad (23')$$

Thus the two points of view agree and, combined, suggest a value of R of 0.9 to 1 fermi. Notice the remarkably high values of ℓ involved in testing high-energy experiments: my ℓ-line of Fig. 8 runs off scale at $\ell = 12$ for 13 GeV/c of beam momentum.

C2. Channels like $\pi^- p \to \Delta^- \pi^+$, as plotted in Fig. 1.

Here the forward peaks are suppressed because exotic exchanges are needed, and Trilling suggests that R (and $\ell = kR$) is probably decreased. Let's take a closer look at the original four reactions of Fig. 2, which SU(3) says should all be equal:

$$\tfrac{1}{3}\sigma(\pi^- p \to \Delta_\delta^- \pi^+), \text{ at 2 GeV/c, } k = 670 \text{ MeV/c} \qquad (24)$$

$$\sigma(\text{"} \to \Sigma_\delta^- K^+), \qquad (25)$$

$$\sigma(K^- p \to \Sigma_\delta^- \pi^+), \text{ at 2 GeV/c, } k = 420 \text{ MeV/c} \qquad (26)$$

$$\sigma(\text{"} \to \Xi_\delta^- K^+), \qquad (27)$$

where the subscript δ stands for the $3/2^+$ decuplet.

In Fig. 9 (Trilling's Fig. 1) he plots a collection of observed cross sections, with a curve drawn through reaction (25) which is the best known. What value of ℓ does one now insert into Eq. (20) to scale from reaction (25) to the other three? Equations (23) or Fig. 8 suggest $\ell_{max} = 4$ for nonexotic exchange, but as expected that overcorrects this set of reactions. We try reducing R from 1 F to about 3/4F, and ℓ_{max} from 4 to 3. That still overcorrects. Then we realize that since large ℓ is ruled out by exotic exchange, and cannot dominate the reaction, perhaps we should scale with an average ℓ, say 2 instead of the 3 we just tried. That works very well (see Fig. 10).

[Trilling does not in fact scale with $\ell = 2$. Instead of the full barrier expressions (10.1) he uses the threshold limits (10.2) which are too extreme. Consequently he needs an average ℓ of only unity. This question can be resolved in the near future, since partial wave analyses of reactions (24) and (26) are soon to be published.]

Trilling goes on to apply his recipes to many reactions, including photoproduction, and the results are very encouraging. I conclude that there has been notable progress in the application of SU(3) to hadronic interactions, and suggest that you read Trilling's paper.

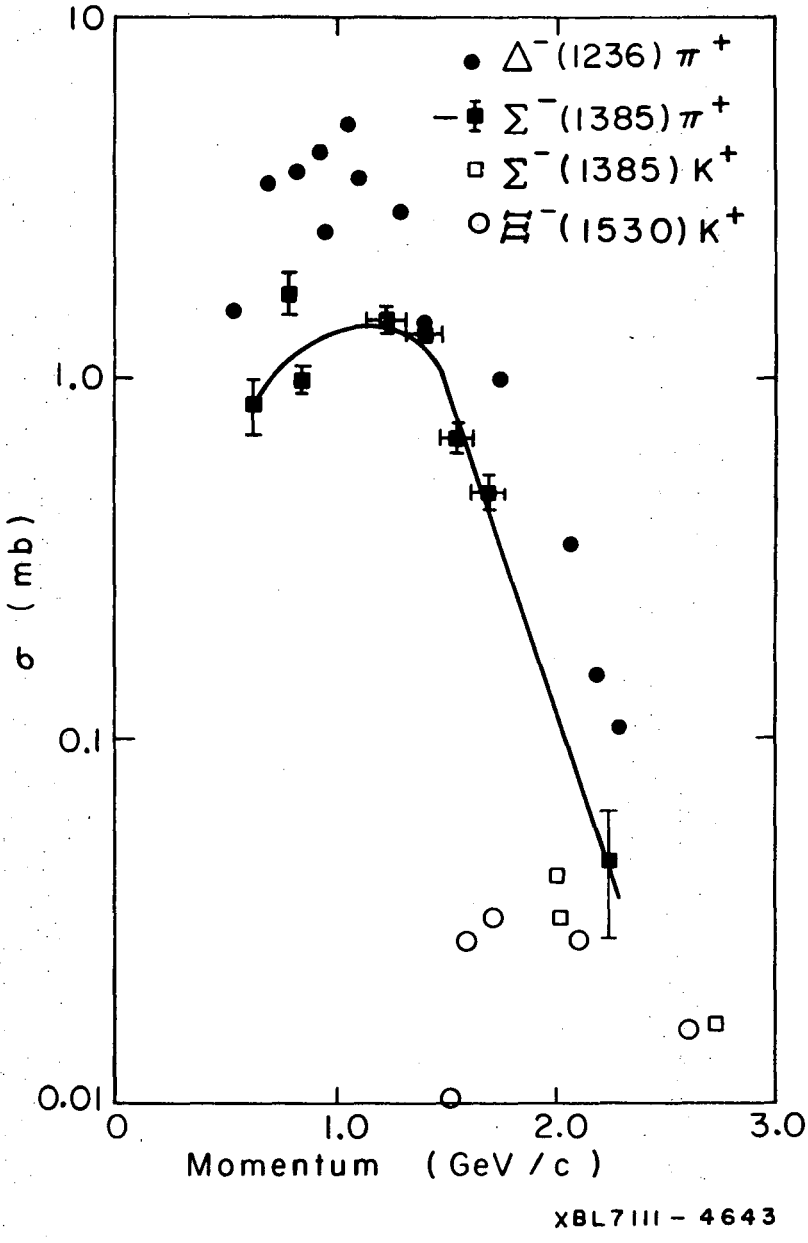

Fig. 9. Cross sections for reactions (24) through (27), which are the same as appeared in Fig. 1. Solid curve is hand-drawn through the $\Sigma\delta\pi^+$ data, which have the smallest errors. This is Trilling's Fig. 1.

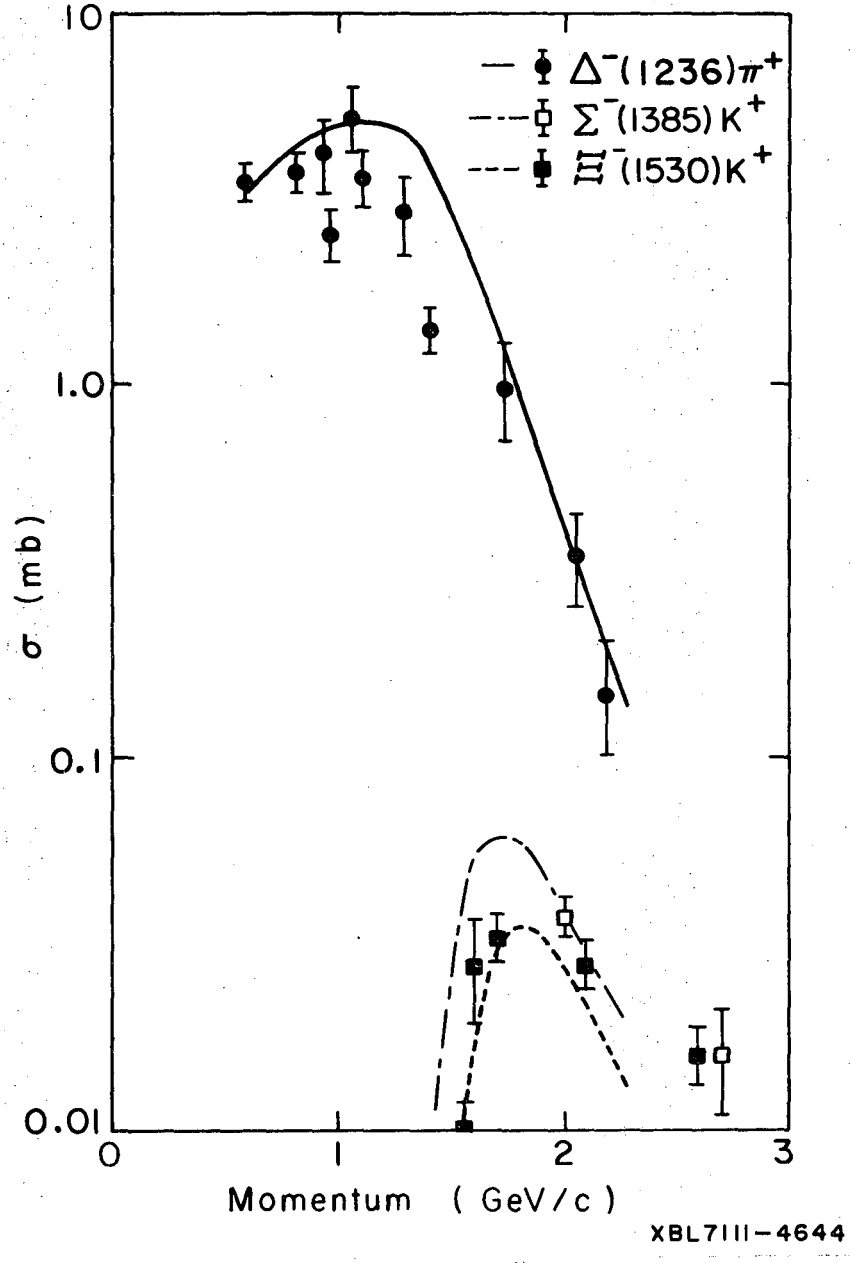

Fig. 10. The curve of Fig. 9 has been scaled according to Eq. (19) to give agreement with the other three cross sections. The effective value of ℓ is 2 or 1 (see text). This is Trilling's Fig. 2.

II. S-WAVE SCATTERING OF $\pi\pi$ AND $K\pi$: THE ϵ AND S^* MESONS

A. The $\pi\pi$ S-Wave Amplitude

1. Summary of Published Papers

Figure 12(a) shows all information published as of the date I am speaking (Dec. 1971). There is agreement that the I-spin zero, S-wave phase shift δ_0^0 rises slowly to 60° at 700 MeV, but as soon as the amplitude enters the strong S-P interference region under the $\rho(765)$ meson, confusion reigns, for the reasons that I shall discuss in B below. Baton et al. could not distinguish between the two solutions plotted (labelled "up" and "down"). Moreover if we look at recent preprints, the situation is not reassuring. If we look ahead at Fig. 12(b), which shows some data that will be published in 1972, we see that Baillon et al. at SLAC are still having ambiguity problems, and that at higher energies the Wisconsin-Toronto group (Caroll 72) is having trouble agreeing with its own earlier solution (Oh 70) based on the first 40% of its data.

The only significant omen in Fig. 12(a) is a lone elasticity limit plotted as a triangle labelled HYAMS 70. This result (from the CERN-Munich-ETH, IC, Hawaii collaboration[10]) shows a sudden rise in the inelasticity at $\bar{K}K$ threshold, and suggests the need for a coupled channel ($\pi\pi$ and $\bar{K}K$) analysis.

An of course, to complete the summary of what is published, the Particle Data Meson Table of last year (April 71) had an S^* entry:

		Branching Fractions	
$\eta_{0^+}(1070)$ or S^*	$I^G(J^P) = 0^+(0^+)$, Γ = 150-300 MeV if resonant	$\pi\pi$	< 65%
		$\bar{K}K$	> 35%

2. The New 7.1-GeV π^+ Experiment of LBL's Group A

Group A decided to invade this disarrayed field with its large 7.1-GeV bubble chamber experiment. (This is the film that Group A had taken to study the splitting of the $A2^+$, and which surprisingly showed no splitting.) The reactions studied for $\pi\pi$ scattering were:

$$\pi^+ p \to \Delta^{++}\pi^+\pi^-$$
$$\to \Delta^{++}K^+K^-.$$

This experiment has the following advantages over earlier ones.
a) More events, and enough $\bar{K}K$ events to permit a two-channel analysis.
b) Better extrapolation to the π pole for the following reason:

The matrix element at the lower vertex of the sketches below involves

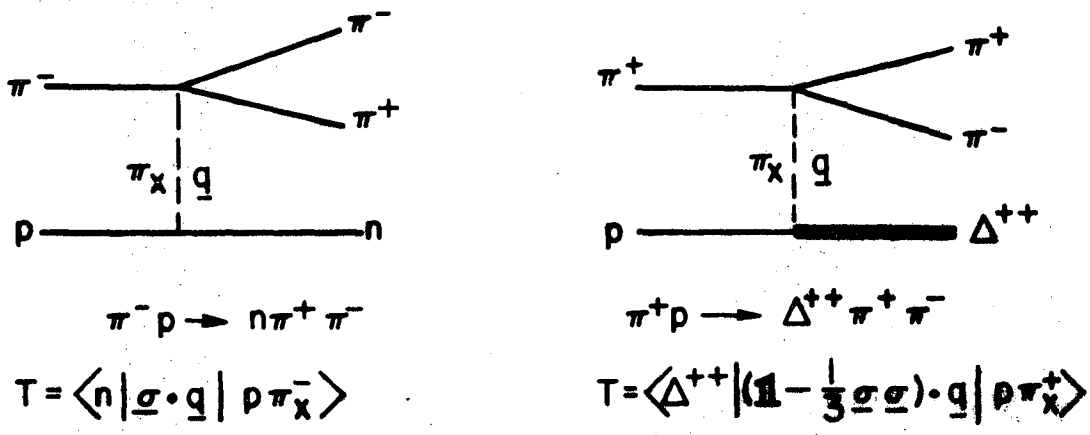

XBL 724-2761

a factor $\underline{q}$, the 3-momentum of the exchanged π. Moreover, if a proton (as opposed to a Δ^{++}) is produced at the lower vertex, $\underline{q}$ goes to zero between the physical region and the π pole. This produces well-known difficulties in the extrapolation, as discussed for example by Kane[11] at the 1970 Philadelphia Conference. A Δ^{++}, however (as opposed to a proton), can emit a real pion, and if the lower vertex involves the production of a Δ^{++} one can extrapolate to the π pole without going near $\underline{q} = 0$. So the Group A experimenters find that linear extrapolations seem to work well.

There is of course also a disadvantage to producing Δ^{++} instead of nucleons: for the same beam energy one cannot get as close to t = 0. But luckily the Group A experiment was at fairly high energy (7.1 GeV/c) so that small values of t are still accessible.

I am not sure which of these two advantages is more important, but Fig. 11 certainly demonstrates that the experiment uncovered stucture never seen before.

Figure 11 is taken from the preprint of Flatté et al.[12] Note the discontinuity in $\langle Y_1 \rangle$ at about 988 MeV (KK threshold) and the associated rise in $\sigma(\bar{K}K)$ and in $\langle Y_2 \rangle$.

These striking features of Fig. 11 permit Flatté et al. to perform a coupled-channel analysis and to arrive at the Argand plot shown. It turns out that the $\eta_{0^+}(1070) = S^*$ is really the $\eta_{0^+}(980 \pm 10)$

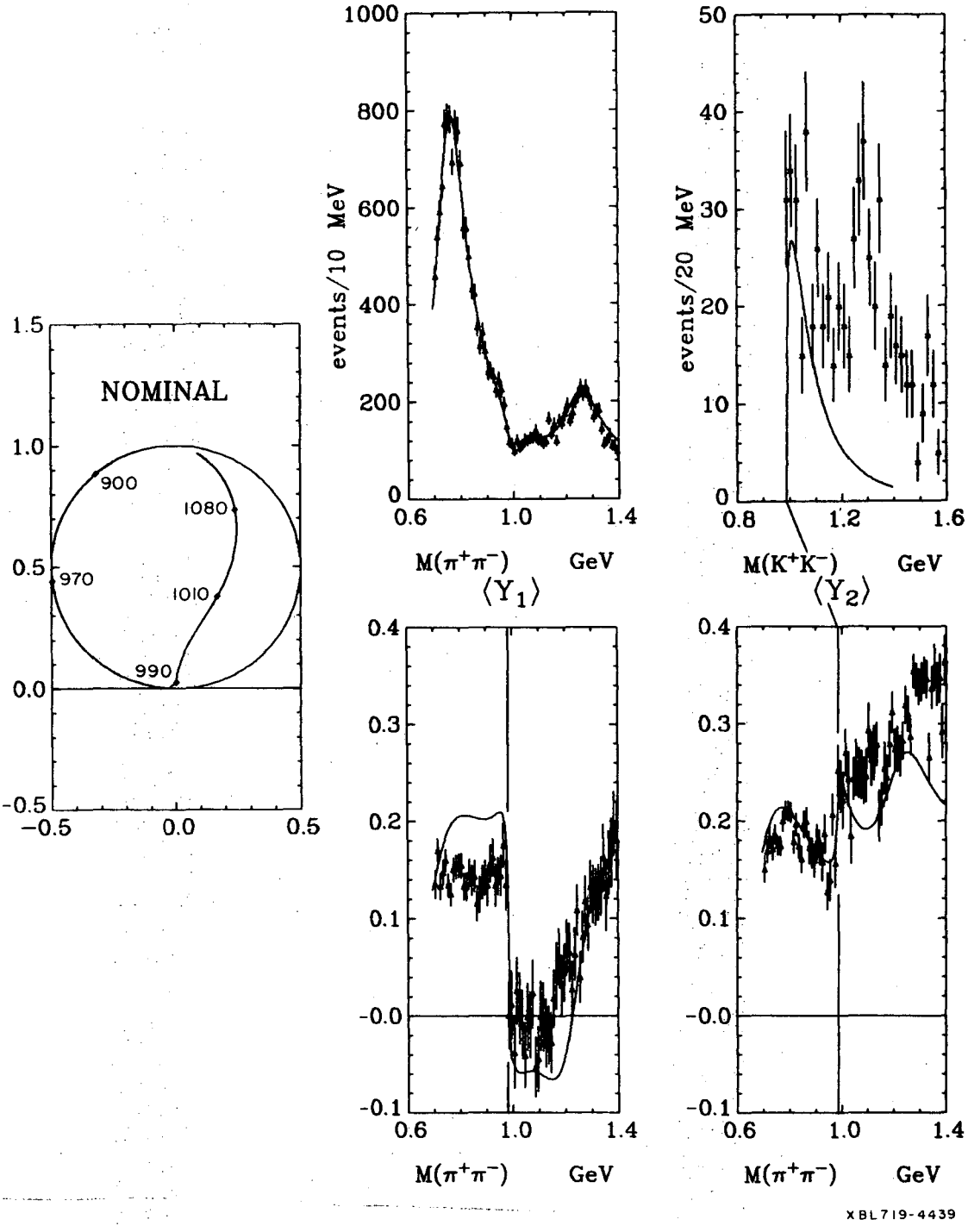

Fig. 11. Number of events and spherical harmonic moments as a function of mass in the reactions $\pi^+p \to \Delta^{++}\pi^+\pi^-$ and $\pi^+p \to \Delta^{++}K^+K^-$ at 7.1 GeV/c. The curves are derived from an OPE approximation which treats the $\pi^+\pi^-$ and K^+K^- systems as final states in the $\pi^+\pi^-$ scattering process. The amplitude includes a ρ-meson and f-meson, and S-wave interaction which includes a constant-phase-shift background and an S^* resonance which couples to both $\pi\pi$ and $K\bar{K}$. The S-wave amplitude is shown on the Argand plot. Since the model fails above 1050 MeV, this amplitude is probably very inaccurate in that region. This is Fig. 1 of Flatté et al., Phys. Letters 38B, 232 (1972).

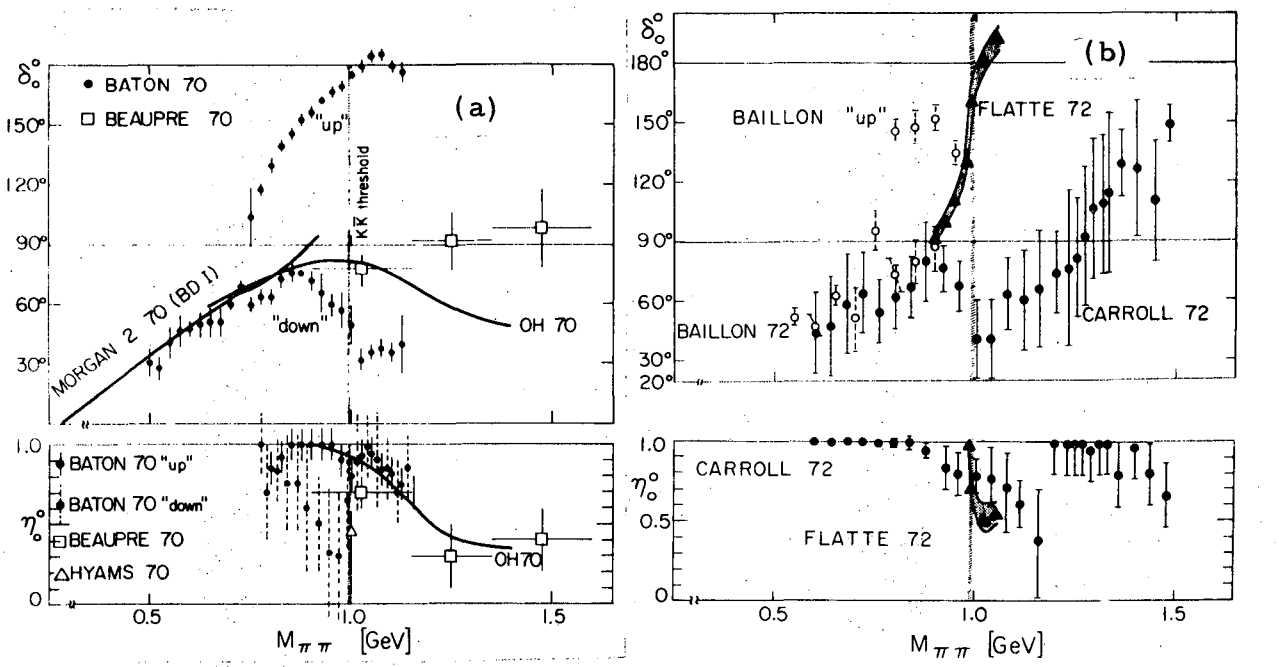

XBL 724-683

Fig. 12(a) The $\pi\pi$ S-wave, I = 0 phase shift parameters, showing some solutions available through 1971. BATON 70 actually presented two "down" solutions; the one we plot allowed for inelasticity, the other corresponded to a purely elastic hypothesis. The new 4π data of ALSTON-GARNJOST 71 show that the $\pi\pi$ channel is essentially elastic up to $K\bar{K}$ threshold; if we had plotted the elastic fit of BATON 70, it would have agreed better with the newer fits in (b).

(b) The $\pi\pi$ S-wave, I = 0 phase shift parameters, as given by three very recent solutions: BAILLON 72, CARROLL 72, and FLATTE 72. Energy-dependent fits are indicated by lines, or (when errors are given) by triangles (indicating the central value in each bin used) and an error band (FLATTE 72). Energy-dependent solutions are indicated with central values and errors; the solutions of BATON 70 are not strictly energy-independent since they were actually determined from smooth curves through the data.

This figure is from Reviews of Particle Properties, Particle Data Group, Physics Letters, April 1972. Complete references are contained therein.

and is coupled comparably to $\pi\pi$ and to $\bar{K}K$. They introduce coupling constants g_π and g_K between the S^* and $\pi\pi$ or $\bar{K}K$, and find

$$g_\pi = 0.2, \qquad g_K = 0.5.$$

But I feel that the most interesting part of the story is yet to come. Turn now to Fig. 12(b), where the solution plotted as an Argand plot in Fig. 11 is plotted as bands of δ_0^0 and of η_0^0. Two comments are in order:

1) In addition to showing the S^* resonance (seen by none of the older solutions) the solution of Flatté et al. rules out the earlier "up" solutions. This has implications on the credibility of "up" solutions for $K\pi$ scattering which I shall discuss under B below.

2) Instead of flapping unpredicatably like a flag in the wind, the solution is now tied down between 900 and 1000 MeV, and one can go back and try to explain the region below 900 MeV.

Note added after I returned to Berkeley:

Serban Protopopescu and his collaborators on the 7.1-GeV/c π^+ experiment have now done a complete 2-channel K-matrix fit to the $\pi\pi$ and $\bar{K}K$ s-waves between 550 and 1150 MeV. Their results will appear as LBL 787 and as a talk by Protopopescu in the Proceedings of the forthcoming 1972 Philadelphia Conference,[13] but they permit me to say that they get a good fit with two poles, the S^* (already reported by Flatte et al.[12]) and the long-sought ϵ meson. Typical positions of these poles are:

$$\epsilon: \quad \sqrt{s} = (600 \pm 70) - i(250 \pm 50), \text{ Sheets II or IV}$$
$$S^*: \quad \sqrt{s} = (980 \pm 7) - i(38 \pm 7), \text{ Sheet II.}$$

(The sheets are defined by: $\text{Im } k_{\pi\pi} < 0$ and $\text{Im } k_{\bar{K}K} > 0$ for II,

$\text{Im } k_{\pi\pi} > 0$ and $\text{Im } k_{\bar{K}K} < 0$ for IV.)

B. The $K\pi$ S-wave amplitude and the "Up-Down" Ambiguity

Finally, I would like to present the present status of $K\pi$ S-wave scattering and discuss the "up-down" ambiguity, which plagues both $\pi\pi$ and $K\pi$ scattering.

The current $K\pi$ situation is summarized in Fig. 13, which we have prepared for the next edition of Reviews of Particle Properties.[4] Apart from the fact that there is no analogy to $\bar{K}K$ threshold, our $K\pi$ Fig. 13 is very reminiscent of our $\pi\pi$ Fig. 12. I now want to explain the ambiguities common to both figures, and shall do so in terms of the multiple branches at the D-wave $K^*(1420)$ plotted in Fig. 13. In this mass region we consider only $S_{1/2}$ and $D_{1/2}$ waves;

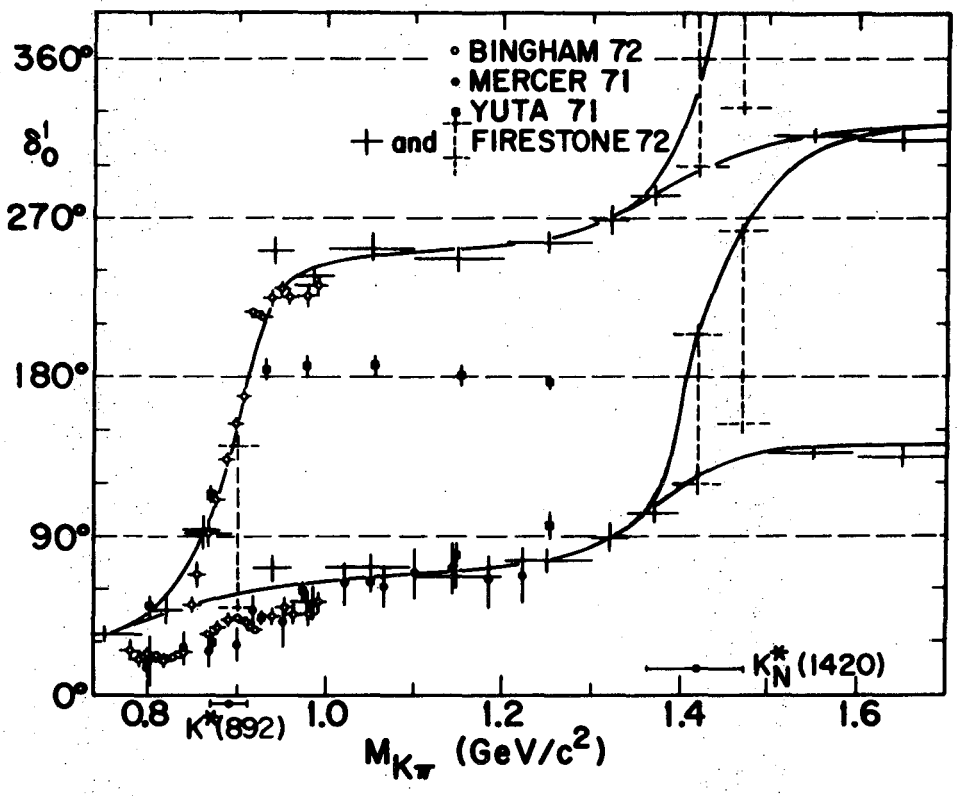

XBL 724-679

Fig. 13. I-spin 1/2 S-wave Kπ phase shift. Taken from Review of Particle Properties, Physics Letters, April 1972. References are contained therein.

then

$$\sigma \propto |S|^2 + 5|D|^2, \ \langle Y_1 \rangle = \langle Y_3 \rangle = 0,$$

and

$$\sigma \langle Y_2 \rangle \propto 4.5 \ \mathrm{Re} S^* D + 3.2 \ |D|^2, \ \sigma \langle Y_4 \rangle \propto |D|^2. \qquad (28)$$

Suppose one takes D as a known resonant amplitude, and solves for S, using only the un-normalized moments $\sigma \langle Y_2 \rangle$ and $\sigma \langle Y_4 \rangle$. S enters only in $\langle Y_2 \rangle$ and only then in the form $\mathrm{Re} S^* D = SD \cos \theta_{SD} \equiv \underline{S} \cdot \underline{D}$.

This situation is sketched in Fig. 14. A constant "real" S ($\approx 100°$ according to FIRESTONE 72) is plotted as a fixed black dot; an ambiguous moving solution S' as an open circle. Lines of constant $\underline{S} \cdot \underline{D}$ lie on a perpendicular to D, running through the "real" S. The general case is plotted in Fig. 14(a). Consider the dashed line OD' parallel to D, drawn from the center of the unitary circle. One can see by inspection that OD' is the bisector of the angle SOS', so that angle θ_D of OD' is the average of the angles θ and θ', which S and S' subtend from the center of the circle with respect to the horizontal. This leads to the well-known result

$$\delta' = 90° - \delta + \theta_D. \qquad (29)$$

Figures 2(b), (c), and (d) show that as D moves through resonance, S' also moves counterclockwise and crosses S near resonance. Moreover, at this crossing point the perpendicular to D is tangent to the unitary circle, so that δ and δ' are insensitive to $\underline{S} \cdot \underline{D}$ and so are badly determined.

Figure 14(e) displays δ' vs θ_D according to (28) for a constant "real" δ of 100°. The errors are plotted assuming a typical error in $\langle Y_2 \rangle$ of ± 0.02.

Far from the D-wave resonance, the data on $\sigma \propto |S|^2 + 5|D|^2$ can sometimes resolve the ambiguity.

There is yet another difficulty, pointed out to me by Christoph Schmid, namely that inadequacies in the model being used to fit the data may cause instabilities in the solution which in turn may throw one "off the track" of the real solution and onto the track of the "mirror."

Consider again Fig. 14(c) where D is about to cross S. If D has the same phase as S, the amplitude

$$T = S + 5 \ D \ P_2 \ (\cos \theta)$$

should go to zero at angles θ such that $P_2(\cos \theta) = -S/5D$. But there will be some intensity measured at these angles, for example, because there are diagrams other than pion exchange, so the model

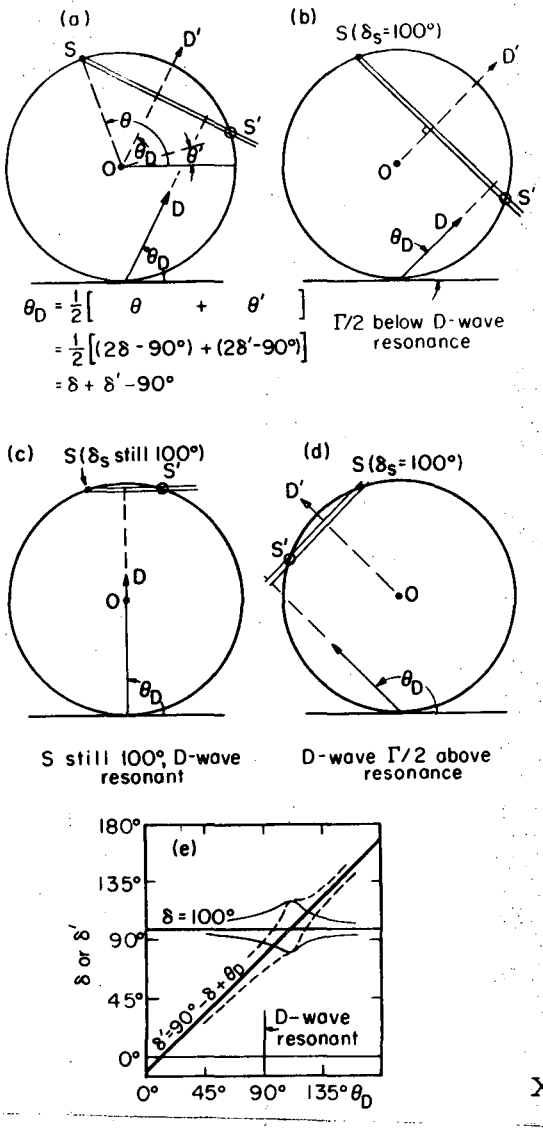

XBL 724-680

Fig. 14. A constant "real" S-wave amplitude is plotted at a black dot with $\delta_0^1 = 100°$. The ambiguous moving S' which gives the same value of $\langle Y_2 \rangle$ is plotted as an open circle. The four cases (a) through (d) are explained in the text. The locus of S' is the 45° line in Fig. 14(e).

cannot fit the data. A χ^2 barrier will grow where S has the same phase as D, with two relative minima on either side. S will then be repelled by D and sit first in the left-hand minimum, then flip to the right-hand one as D crosses S. This is all very annoying, since (for the large S of Fig. 14) it occurs just as S' is also crossing S and one is trying to distinguish solutions on the grounds of continuity.

In the paragraph above I have said "S·D" interference because I wanted to refer to Fig. 14. In actual practice it is the instability in S·P interference which is currently troublesome—specifically the two points at about 860 MeV in Fig. 13, where the $K^*(890)$ P-wave crosses the "down" S solution.

To complete the list of ambiguities, remember that one can never distinguish solutions modulo π.

To illustrate these difficulties, Firestone et al. have drawn many possible paths connecting ambiguous solutions, and we have copied these in Fig. 13. To further illustrate the problem, we have drawn their unique solutions as solid crosses, but drawn their ambiguous ones as pairs of dashed crosses joined by a dashed vertical line. These ambiguities of course occur at $K^*(890)$ and $K^*(1420)$.

All this discussion of ambiguities should make it evident that I would bet strongly on the smoothest track, which in the case of $K\pi$ is the lowest one. It then looks very much like that for $\pi\pi$, where the lowest one has turned out to be favored by Flatté et al.

ACKNOWLEDGMENTS

Almost nothing that I have said is original. I want to thank the friends from whom I have collected these ideas: in particular, George Trilling, Tom Lasinski, Lina Galtieri, Maxine Matison, Stan Flatté, and Serban Protopopescu.

REFERENCES

1. R. D. Tripp et al., Nucl. Phys. B3, 10 (1967).

2. Meschkov, Snow, and Yodh, Phys. Rev. Letters 13, 212 (1964).

3. G. H. Trilling, LBL-522 and Nucl. Phys. B (in press, 1972).

4. Review of Particle Properties, Phys. Letters, April 1972.

5. R. Levi-Setti, in Proc. of the 1969 Lund Intl. Conf. on Elementary Particles (Inst. of Physics, Lund, Sweden).

6. F. von Hippel and C. Quigg, Phys. Rev. B5, 624 (1972).

7. Handbook of Mathematical Function, edited by Abramovitz and Stegun. Natl. Bureau of Standards Applied Math. Series, 55 (US GPO, 1964).

8. D. F. Kane, UCRL-20682 (1971) (unpublished).

9. M. Davier and H. Harari, Phys. Letters 35B, 239 (1970).

10. Hyams, Koch, Lorenz, Lutjens, Ochs, Schlein, Stierlin, Weilhammer, Beusch, Wetzel, Johnson, Stenger, and Wohlmut; in Proc. of the 1970 Philadelphia Conf. on Exptl. Meson Spectroscopy, edited by Baltay and Rosenfeld (Columbia, 1970).

11. Gordon Kane, pg. 1 of the 1970 Philadelphia Proceedings (see Ref. 10).

12. Flatté, Alston-Garnjost, Barbaro-Galtieri, Friedman, Lynch, Protopopescu, Rabin, and Solmitz, Phys. Letters 38B, 232 (1972).

13. Protopopescu, Alston-Garnjost, Barbaro-Galtieri, Flatté, Friedman, Lasinski, Lynch, Rabin, and Solmitz; LBL-787 and in Proc. of the 1972 Philadelphia Conf. on Exptl Meson Spectroscopy, edited by Baltay and Rosenfeld (Am. Inst. of Phys., to be published, 1972).

TECHNICAL INFORMATION DIVISION
LAWRENCE BERKELEY LABORATORY
UNIVERSITY OF CALIFORNIA
BERKELEY, CALIFORNIA 94720